JCI insight

Stem cell transplantation impairs dendritic cell trafficking and herpesvirus immunity

Carol A. Wilke, … , Bethany B. Moore, Xiaofeng Zhou

JCI Insight. 2019. https://doi.org/10.1172/jci.insight.130210.

Research In-Press Preview **Immunology** **Inflammation**

Long-term survivors post hematopoietic stem cell transplantation are at high risk of infection which accounts for one-third of all deaths. Little is known about the cause of inferior host defense after immune cell reconstitution. Here, we exploited a murine syngeneic bone marrow transplantation (BMT) model of late infection with gammaherpesvirus 68 (MHV-68) to determine the role of conventional dendritic cell (cDC) trafficking in adaptive immunity in BMT mice. Post infection, the expression of chemokine *Ccl21* in the lung is reduced and the migration of cDCs into lung draining lymph nodes (dLNs) is impaired in BMT mice, limiting the opportunity for cDCs to prime Th cells in the dLNs. While cDC subsets are redundant in priming Th1 cells, *Notch2* functions in cDC2s are required for priming increased Th17 responses in BMT mice and cDC1s can lessen this activity. Importantly, Th17 cells can be primed both in the lungs and dLNs, allowing for increased Th17 responses without optimum cDC trafficking in BMT mice. Taken together, impaired cDC trafficking in BMT mice reduces protective Th1 responses and allows increased pathogenic Th17 responses. Thus, we have revealed a previously unknown mechanism for BMT procedures to cause long-term inferior immune responses to herpes viral infection.

Stem cell transplantation impairs dendritic cell trafficking and herpesvirus immunity

Carol A. Wilke[1], Mathew M. Chadwick[1], Paul R. Chan[1], Bethany B. Moore [1,2] and Xiaofeng Zhou[1]*

1. Division of Pulmonary and Critical Care Medicine, Dept. of Internal Medicine, University of Michigan Medical School, Ann Arbor, MI, USA.
2. Dept. of Microbiology and Immunology, University of Michigan, Ann Arbor, MI, USA.

*Corresponding author:

Xiaofeng Zhou, PhD

Department of Internal Medicine

4062 BSRB

109 Zina Pitcher Place

Ann Arbor, MI 48109-2200

Phone: 734-647-9968

Email: xiazhou@umich.edu

ORCID: 0000-0003-3096-409X

Conflict of interest statement

The authors have declared that no conflict of interest exists.

Abstract

Long-term survivors post hematopoietic stem cell transplantation are at high risk of infection which accounts for one-third of all deaths. Little is known about the cause of inferior host defense after immune cell reconstitution. Here, we exploited a murine syngeneic bone marrow transplantation (BMT) model of late infection with gammaherpesvirus 68 (MHV-68) to determine the role of conventional dendritic cell (cDC) trafficking in adaptive immunity in BMT mice. Post infection, the expression of chemokine *Ccl21* in the lung is reduced and the migration of cDCs into lung draining lymph nodes (dLNs) is impaired in BMT mice, limiting the opportunity for cDCs to prime Th cells in the dLNs. While cDC subsets are redundant in priming Th1 cells, *Notch2* functions in cDC2s are required for priming increased Th17 responses in BMT mice and cDC1s can lessen this activity. Importantly, Th17 cells can be primed both in the lungs and dLNs, allowing for increased Th17 responses without optimum cDC trafficking in BMT mice. Taken together, impaired cDC trafficking in BMT mice reduces protective Th1 responses and allows increased pathogenic Th17 responses. Thus, we have revealed a previously unknown mechanism for BMT procedures to cause long-term inferior immune responses to herpes viral infection.

Introduction

Hematopoietic stem cell transplantation (SCT) is a curative therapy for many malignant, autoimmune and inherited disorders; however, infectious complications are a leading cause of morbidity and non-relapse mortality post-SCT (1, 2). SCT conditioning disrupts the natural barriers of the epithelium and mucous membranes and destroys or severely weakens the host immune system (3). The recovery of T lymphocyte counts, especially $CD4^+$ T cells, predicts better survival and reduced risk of infections (1, 4-8). Regeneration of naïve $CD4^+$ T cells occurs from 4 to 24 months in patients less than 45 years (9). However, patients who survive more than 2 years after allogeneic SCT are still at considerably higher risk of infection than the age-matched general population (10-12) and infectious diseases account for one-third of all deaths (13). Infections are less common in autologous SCT recipients, nevertheless infectious diseases contribute to one-third of late non-relapse mortality among this group of patients (14), suggesting that even in the absence of chronic graft-versus-host disease (cGVHD) and immunosuppressive therapy, autologous SCT recipients still suffer from long-term immune dysfunction.

The inferior immune defense against infections after full reconstitution of T lymphocytes is not well understood, but may be due to the reconstitution and activation of T cells in a SCT-altered microenvironment that differs from normal conditions (9). A conditioning-induced proinflammatory cytokine storm that lasts for weeks post-SCT (15-17), shapes the antigen-specific T lymphocyte repertoire and Th cell phenotypes, *i.e.* Treg, Th1, Th2, and Th17 (18). Dendritic cells (DCs), a potent population of professional antigen-presenting cells (APCs) that activate and define T cell responses, reconstitute rapidly post-transplant but with prolonged skewing of cell subsets (16). Furthermore, SCT conditioning damages the fibroblastic reticular cells and their expression of CCL21 in secondary lymphatic organs (19-21). CCL21 is essential for lymph nodes (LNs) to recruit naïve T cells (22) and DCs (23). We recently demonstrated that

cytokine production of APCs is dysregulated in response to infection with herpesvirus and causes a Th17 phenotype in a mouse syngeneic bone marrow transplant (BMT) model (24). Clearly, the unique microenvironmental conditions post-SCT play an important role in shaping recipients' immune reconstitution.

Reactivations of latent human herpesviruses (HHVs) are common during the early post-engraftment phase and throughout late post-engraftment (1, 25, 26). Cytomegalovirus (CMV), human herpesvirus 6 (HHV-6), Epstein-Barr virus (EBV) and varicella zoster virus (VZV), are among the most frequently reactivated viruses post-SCT. HHV infections after SCT can lead to life-threatening diseases such as pneumonitis, encephalitis or post-transplant lymphoproliferative disease (25). In addition, we and others have recently revealed a strong association between reactivations/infections with herpes or respiratory viruses and the risk of high mortality "noninfectious" pulmonary complications post-SCT, such as idiopathic pneumonia syndrome and bronchiolitis obliterans syndrome (27-30).

To better understand the mechanisms underlying the pathogenesis of herpes viral infections post-SCT, we modelled the infection by inoculating murine gammaherpesvirus 68 (MHV-68), a mouse homolog of EBV and Kaposi's sarcoma-associated herpesvirus, into syngeneic BMT recipients (BMT mice) intranasally 5 weeks post-BMT. Note that innate immune cell numbers are restored at 3 weeks post-BMT (31) and T lymphocyte regeneration in the thymus (19) and reconstitution in the lung and spleen are complete at 5 weeks (32) in syngeneic BMT mice. This model allows us to study transplant-related alterations to immune cell function without the added complication of allo-immune responses. However, even after full immune cell reconstitution, BMT mice can still experience impaired innate and adaptive immunity to bacterial or viral infection [reviewed in (33)]. BMT mice developed severe pneumonitis and lung fibrosis three weeks post-infection with MHV-68, whereas infected non-BMT mice showed no pathology (24, 34, 35). This lung pathology was driven by pathogenic Th17 responses with weakened

protective Th1 responses (24). APCs isolated from the lungs of BMT mice not only produce increased levels of pro-Th17 cytokines such as IL-6, TGF-β and IL-23, but surprisingly also produce high levels of the pro-Th1 cytokine IL-12. This is in contrast to the suppressed anti-viral Th1 responses in vivo (24). Lung-resident conventional DCs (cDCs) are the most efficient APCs in the lung in sampling air-borne and blood-borne pathogens (36). After taking up and processing antigens, cDCs are thought to migrate into the mediastinal dLN to present antigens to and prime naïve T cells (37). There are two major lineages of cDCs in the lung, i.e. type 1 cDCs (cDC1s) expressing CD8α, CD24, XCR1 and CD103, and cDC2s expressing CD4, Sirpα, and CD11b (38, 39). cDC1s are responsible for cross-presenting antigens to $CD8^+$ T cells for antiviral immunity, while cDC2s have been shown to support type 2 T helper (Th2) and type 17 (Th17) cell responses (39).

Here we report underlying mechanisms for the insufficient protective, yet pathogenic immune response to infection with gammaherpesvirus in syngeneic BMT mice after full immune reconstitution. We found that although lung cDCs of BMT mice are potent in inducing Th1 responses *ex vivo*, they are unable to induce strong Th1 responses in vivo due to their impaired migration into lung dLNs to prime T cells after infection. Furthermore, a subset of *Notch2* functionally dependent cDC2s are solely responsible for priming Th17 cells, while cDC1s suppress excessive Th17 responses. Our data also suggest that impaired migration of cDC2s allows for increased Th17 responses in BMT mice, as cDC2s can locally prime Th17 cells in the lungs without entering into the dLNs. Thus, our study sheds light on understanding the vulnerability of SCT recipients to infections even after immune reconstitution.

Results

APCs from lungs of BMT mice are potent in stimulating both Th1 and Th17 responses

We previously reported, and confirm again here, that BMT mice display reduced protective Th1 responses and increased pathogenic Th17 responses in the lungs 7 days post intranasal inoculation with 5 x 10^4 pfu MHV-68 (**Figure 1A**; 24). The BMT mice develop severe pneumonitis and lung fibrosis 3 weeks post infection, and IL-17A is essential for the development of the lung pathology (24, 34). Surprisingly, APCs isolated from BMT mice express higher levels of the pro-Th1 cytokine IL-12p35 than APCs from non-BMT mice, even though the Th1 responses in the BMT mice are decreased in vivo (24).

To determine if APCs from BMT mice are capable of stimulating potent Th1 as well as Th17 responses, we isolated $CD11c^+$ APCs (including macrophages and DCs) and $CD4^+$ T cells from the lungs of infected BMT mice and co-cultured them (1:10 ratio) for four days. Concentrations of both IFN-γ and IL-17A in the supernatant of the co-cultures with BMT APCs were significantly higher than that with non-BMT APCs (**Figure 1B**). Indeed, increased mRNA expression levels of both pro-Th1 and pro-Th17 cytokines, i.e. *Il12a*, *Il6* and *Il23a*, were found in co-cultures with BMT APCs compared to non-BMT APCs (**Figure 1C**). Thus, APCs from MHV-68-infected BMT mice are capable of stimulating T cells to produce high levels of IFN-γ in vitro.

DC migration is impaired in lungs of BMT mice

The discrepant results between the in vitro and in vivo studies suggest that APCs from BMT mice can fully interact with and stimulate CD4 T cells in vitro, but they may not have optimum interactions with T cells in vivo. We thus hypothesized that cDCs are impaired in migrating from the lungs to the draining lymph nodes (dLN) in BMT mice to prime naïve T cells. We first enumerated cDCs in lungs based on their high expression of CD11c and MHC class II molecules, and low levels of siglec F and CD64, which are markers for macrophages and

monocyte-derived DCs (40-42) (**Figure 2A**). These cDCs can be further identified as cDC1 and cDC2 cells based on their discrepant expression levels of CD103/CD24 and CD11b (**Figure 2A**). Migratory cDCs (mDCs) moving from the lung to the dLN can also be classified based on their high expression of MHC class II molecules and high or intermediate levels of CD11c (**Figure 2A**). In naïve mice or mice two days post infection (dpi) with MHV-68, similar number of cDC1s are present in the lungs of control (non-BMT) and BMT recipients (**Figure 2B**). There are fewer CDC2s in the lungs of non-BMT mice at day 0, but by 2 dpi, numbers are similar to each other (**Figure 2B**). However, fewer cDC1s or cDC2s remain in the lungs of normal mice compared to BMT recipients at 3 dpi (**Figure 2B**), suggesting that in normal mice more cDCs emigrate out of the lungs than in BMT mice during the first 2-3 dpi with MHV68. In agreement with more cDCs remaining in the lungs in BMT mice, there are significantly less migratory cDC1s and cDC2s in the dLNs in BMT mice at 3dpi with MHV-68 (**Figure 2B**).

To track the migration of cDCs from the lung to the dLN, non-BMT or BMT mice at 2 dpi with MHV-68 were instilled with 5 mM CFSE via oropharyngeal aspiration to label all the cells in the lungs, and at 18 hours post CFSE instillation, dLNs were harvested to enumerate $CFSE^+$ mDCs by flow cytometry analysis (**Figure 2C**). Both the percentages and absolute numbers of $CFSE^+$ cDC1s and cDC2s were significantly reduced in BMT dLNs comparing to the non-BMT mice (**Figure 2C** and **D**). Taken together, our data demonstrate that the migration of lung cDCs to the dLN is impaired in BMT mice.

Reduction in Th1 cell differentiation and cellularity in dLNs in BMT mice

To examine whether impaired cDC migration affects subsequent priming of Th cells in lung dLNs, we enumerated and characterized the cells in the dLNs at 7 dpi with MHV-68. Indeed, the absolute numbers of Th1 cells in the dLNs of BMT mice are significantly reduced (**Figure 3A**), consistent with limited Th1 responses in BMT mice. Notably, although fewer in cell counts, the percentages of Th1 cells within the dLNs are comparable between non-BMT and BMT mice

(**Figure 3A**), suggesting that the cDCs of BMT mice are potent in priming Th1 responses once reaching the dLNs. While the numbers of Th17 cells are comparable between normal and BMT mice in the dLNs, the Th17 cells of BMT mice make up a larger percentage of the population than that in non-BMT mice (**Figure 3B**), further confirming a Th17-skewed response. It has been previously reported that both allogeneic and congeneic BMT reduces steady state cellularity in LNs after immune reconstitution and that BMT mice generate poor responses to bacterial and viral infections (19-21). Similarly, we also found that there is about a three-fold reduction in total cell numbers in BMT lung dLNs at 7 dpi, with significantly fewer mDCs, $CD4^+$ Th cells, $CD8^+$ T cells and B cells in the BMT dLNs (**Figure 3C**).

BMT down regulates the expression of chemokine *Ccl21* in the lung and dLN but does not affect the surface expression of CCR7 on cDCs

CC-chemokine receptor 7 (CCR7) is essential for mature cDCs to sense and follow the gradient of CCL21 towards and into the lumen of lymphatic vessels leading to dLNs (43). Interestingly, the expression of CCR7 on lung cDCs is similar between non-BMT and BMT mice at 2 dpi when activated lung cDCs are ready to migrate (**Figure 4A**). There are three distinct *Ccl21* genes in the mouse. *Ccl21a* encodes CCL21Ser and is predominantly expressed in lymphoid organs, while *Ccl21b* and *Ccl21c* both encode CCL21Leu and are predominantly expressed in nonimmune organs, such as the lung (44). CCL19 is the other ligand for CCR7, and is also predominantly present within the dLNs (45). We found that the expression levels of *Ccl21a* and *Ccl21b/c* are reduced in the lungs of BMT mice at 3 dpi (**Figure 4B**), consistent with the observation that cDCs stall in the lungs in BMT mice after infection with MHV-68. We also note that levels of *Ccl21a* and *Ccl21b/c* transcripts are similar between the dLNs of non-BMT and BMT mice prior to infection and at 3 dpi (**Figure 4B**); however, both BMT and non-BMT dLNs show reduced transcription of *Ccl21* at 7 dpi, but BMT dLNs show greater reduction (**Figure 4B**). To further determine the cells producing CCL21 in the lungs, we have performed multiple-

color immunofluorescence staining of lung frozen sections. Labelling of CD90.2 protein identifies lymph vessels in the lung (46). Similar to previous studies [reviewed in (47)], we found that CCL21 protein is exclusively expressed in lymphatic endothelial cells in the lung prior to infection (data not shown) and at 3 dpi (**Figure 4C**). Importantly, the number of $CD11c^+$ cells, presumably cDCs, within or in contact with lymph vessels is reduced in BMT lungs at 3 dpi (**Figure 4C**). These observations indicate that the impaired cDC migration in BMT mice is not due to the regulation of CCR7 on the cDC cell surface, but rather is likely due to insufficient production of CCL21 in the lungs.

Disparate functions of cDC1s and cDC2s in priming Th17 differentiation

As shown above, the impaired trafficking of cDCs explains the reduction of Th1 responses in BMT mice after infection with MHV-68; however, it is difficult to explain the increased pathogenic Th17 responses in the lungs of BMT mice since similar numbers of Th17 cells were activated in the dLNs of both non-BMT and BMT mice (**Figure 3B**). We thus wanted to tackle this question by determining the function of each cDC subset in priming Th1 and Th17 cells after infection with MHV-68. *Batf3* is required for the development of cDC1s, and mice deficient in *Batf3* have defective $CD8^+$ T cell responses to viral pathogens (48, 49). As expected, BMT mice receiving bone marrow from *Baft3*$^{-/-}$ mice (*Baft3*$^{-/-}$ BMT) do not develop cDC1s after reconstitution of immune cells (**Figure 5A**). *Notch2* is critical for a subset of cDC2s in the gut and spleen necessary to prime Th17 responses, but interestingly, conditional knockout of *Notch2* in CD11c-expressing cells (*Notch2*^{cKO}) did not reduce the numbers of cDC2s in the lung (50, 51). In agreement with these findings, BMT mice receiving *Notch2*^{cKO} bone marrow have abundant cDCs in their lungs (**Figure 5A**). Percentages of cDC2s in *Notch2*^{cKO} BMT mice are similar to non-BMT mice, but are slightly reduced compared to WT BMT. As expected, *Notch2*^{cKO} BMT mice have reduced percentages (**Figure S1A**) and numbers of cDC2s (**Figure S1B**) in the spleen. Furthermore, *Notch2*^{cKO} BMT mice fail to develop splenomegaly three

weeks after infection with MHV-68 (**Figure S1C**), due to a failure in stimulating the expansion of CD4 T cells and B cells in the spleen (**Figure S1D**). Thus, unlike in the spleen, *Notch2* function does not appear to be required for the development or survival of cDC2s in the lung, but the role of *Notch2* in cDC2s during the priming of Th responses against lung infection is not known.

Deficiency of *Batf3* or *Notch2* in BMT mice does not affect the percentage or absolute numbers of Th1 cells in the lungs or dLNs of BMT mice at 7 dpi (**Figure 5B**), suggesting that neither cDC1s nor *Notch2* functionally dependent cDC2s are solely required for Th1 responses after MHV-68 infection. In contrast, *Notch2* deficiency, presumably specific to cDC2s, diminishes the increase in Th17 responses to MHV-68 infection in BMT mice (**Figure 5C**). These data suggest that *Notch2* function is required by cDC2s for increasing Th17 responses in BMT mice. Previous studies have shown conditional deletion of *interferon regulatory factor 4* (*Irf4*) in cDCs selectively diminishes a lung-resident $CD11c^{hi}$ $CD11b^{+}SIRPa^{+}CD24^{+}$ DC subset and causes reduction in both Th17 responses (52) and Th2 responses (53, 54) in the lungs. Similarly, we find that BMT mice with IRF4 deficiency in cDCs failed to increase Th17 responses after infection with MHV-68 (**Figure S1E**). Loss of cDC1s in *Baft3*$^{-/-}$ BMT mice caused further increased Th17 responses in BMT mice (**Figure 5C**), suggesting that the presence of cDC1s suppress Th17 responses. Interestingly, lifting the suppressive function of *Batf3* in non-BMT mice does not increase Th17 responses (**Figure S2**), presumably because cDC2s in non-BMT mice are not activated by MHV-68 infection, which is evidenced by low production levels of pro-Th17 cytokines (**Figure 1C**). Despite the importance of cDCs in anti-viral infections (48, 49), deficiency in either *Batf3* or *Notch2* in cDCs does not have an impact on viral lytic replication at 7 dpi (**Figure S3**). Taken together, our data demonstrate that *Notch2* function in cDC2s is required for the increased Th17 responses while presence of cDC1s suppress Th17 responses in BMT mice after infection with MHV-68.

Migration of cDC2s into lung dLN is not required for Th17 responses in the lung

The migration of both cDC1s and cDC2s into the dLNs is impaired in a similar manner (**Figure 2**), yet the Th1 and Th17 responses in the lungs of BMT mice are differentially regulated, suggesting that cDC trafficking has different impacts in priming Th1 or Th17 cells. To test this possibility, we performed a BMT using bone marrow cells from *CCR7*$^{-/-}$ donors, so that after reconstitution, the DCs and T cells in the recipient mice will not respond to CCL21. As expected, *CCR7*$^{-/-}$ to WT BMT mice showed minimal Th1 responses in the lungs and dLNs at 7dpi (**Figure 6A**). Surprisingly, the percentages and numbers of Th17 cells in the lungs of *CCR7*$^{-/-}$ to WT BMT mice remained as high as those of WT BMT mice (**Figure 6B**). Also similar to WT BMT mice, *CCR7*$^{-/-}$ BMT mice have significantly higher percentages but comparable numbers of Th17 cells in their dLNs as non-BMT mice (**Figure 6B**). The sphingosine 1-phosphate (S1P) receptor agonist FTY720 blocks the egress of lymphocytes, so the migration of both activated and naïve T cells to sites of inflammation is blocked about 10-12 hours after application of FTY720 (55-57). Furthermore, FTY720 increases blood-borne DCs and reduces DCs in LNs and spleen (58). Therefore, the activated Th cells found in the lungs are presumably primed locally from the naïve T cells that arrived in the lungs before the administration of FTY720. We administered FTY720 1mg/kg/day via intraperitoneal injection starting 3 dpi, and as expected, the total T cells and CD4^{+} T cells in the lung are reduced at 7dpi (**Figure S3A** and **B**). Although the absolute numbers of Th1 and Th17 cells are much lower in FTY720 treated BMT mice (**Figure S3C** and **D**), the percentage of Th cells remain unchanged after FTY720 treatment (**Figure S3E** and **F**). Thus, both data strongly suggest that cDC2s can prime Th17 responses both in the lungs and dLNs of BMT mice and CCR7-dependent migration into the dLNs is not absolutely required for cDC2s to prime Th17 responses, while cDC trafficking to the dLN is essential for priming strong Th1 responses.

Discussion

SCT recipients are at high risk of infection even long after immune reconstitution. We have determined impaired cDC trafficking is an underlying cellular mechanism responsible for the reduced protective Th1 responses to herpesviral infection by exploiting a murine syngeneic BMT model of late infection with MHV-68. The impaired cDC trafficking in BMT mice limits the opportunity for cDCs to prime Th cells in the dLNs. Furthermore, *Notch2* function in cDC2s is required for the increased Th17 responses in BMT mice while cDC1s can partially suppress this activity. Importantly, Th17 cells can be primed both in the lungs and dLNs, and thus allow for increased pathogenic Th17 responses even when the migration of cDCs to dLNs is impaired.

The interaction between CCR7 on cDCs and CCL21 protein orchestrate nearly every step of cDC migration to dLNs [reviewed in (47)]. This interaction first guides mature cDCs to follow the gradient of CCL21 towards and into the lumen of lymphatic vessels in infected tissues (43). Once inside, cDCs first crawl along the vessel wall guided by the CCL21 gradient towards collecting lymphatic vessels (59) and then are passively transported by the lymph flow into lymph nodes (60). Cells travelling within the afferent lymph are drained into the LN subcapsular sinus, where CCL21 gradients once again guide cDC migration into the LN parenchyma (61). We found that the cell surface expression of CCR7 on cDCs is not altered by BMT (**Figure 4A**), but the expression of *Ccl21* in the lung is down regulated at 3 dpi (**Figure 4B**). Together with the observation that reduced numbers of $CD11c^+$ cells are present within or in contact with lymphatic vessels in the lungs of BMT mice (**Figure 4C**), we propose that the initial steps of recruiting cDCs into lymphatic vessels in the lung are dysregulated in BMT mice. Future studies are required to understand the cellular and molecular events involved in cDC trafficking that are dysregulated in BMT recipient lung tissue.

It has been long recognized that the dLNs are small and disorganized in BMT recipients, and BMT mice generate poor responses to bacterial and viral infections (19-21, 62). The levels of

CCL21 protein in dLN stroma have previously been reported to be reduced in BMT mice at steady-state (19, 21), but we did not detect such a reduction of *Ccl21* at the transcription level (**Figure 4B**). A transient down regulation of chemokine production within dLNs was observed in both non-BMT and BMT dLNs at 7 dpi, which has been reported to help orchestrate local cellularity and minimize competition for space and resources in activated lymphoid tissues (63). BMT dLNs reduce their production of *Ccl21* at 7 dpi more dramatically than non-BMT dLNs (**Figure 4B**). CCL21 is also essential for recruiting naïve T cells into LNs (22). It is thus likely that the down regulation of *Ccl21* after the flush of incoming cDCs reduces the recruitment of naïve T cells, and contributes to low cellularity of T cells as well as B cells in the dLNs of BMT mice.

Defects in cDC trafficking have been implicated in diseases. For example, ASAP1 protein regulates matrix degradation and cDC migration through its involvement in actin and membrane remodeling (64). Individuals with genetic variants that reduce the expression of *ASAP1* are associated with susceptibility to *Mycobacterium tuberculosis*, due to the impaired migration of *M. tuberculosis*-infected cDCs (64). In patients with chronic obstructive pulmonary disease (COPD), the functions of DCs are somewhat controversial. Several studies found that DCs accumulate in the small airways (65, 66), and drive natural killer cytotoxicity to kill lung epithelial cells (67). However, such increases in DCs in COPD small airways were not detected in another study (68).

The understanding of the division of labor among the different lung DC subsets has rapidly expanded in recent years. The cDC2 subset appears to be heterogeneous, as they support both Th2 responses to house dust mite (41) and Th17 responses to lung fungal infection with *Aspergillus fumigatus* (52). Further studies found that *Klf4* is required by a set of cDC2s to sustain Th2 responses to *Blomia tropicalis* mites (69), while *Notch2* is required by cDC2s for Th17 responses in defense against *Citrobacter rodentium* in spleen and intestine (50, 51). Since

Notch2 deficiency does not cause reduction of cDC2 cell numbers in the lung (50, 51), whether or not the function of *Notch2* is required for Th17 responses in the lung was not defined. Here we demonstrated that *Notch2* is indeed required for Th17 responses to MHV-68 infection in BMT mice (**Figure 5C**). Surprisingly, cDC2s can prime Th17 cells both in the infected lungs and the dLNs, as evidenced in *CCR7*$^{-/-}$ or FTY720-treated BMT mice (**Figure 5** and **Figure S3**). The precise sites of interaction between cDC2s and Th cells are not yet determined. While we have not noticed well-structured tertiary lymphoid follicles in the lungs of BMT mice after infection, there is a large amount of lymphocyte infiltration that organizes in a patchy manner which may provide unique niches for cDC2s to prime Th cells (34).

Mouse cDC1s are required for cross-presenting antigens to CD8$^+$ T cells for antiviral and antitumor immunity (48, 49). Lung cDC1s can prime both Th1 and Th17 responses in vitro (70), but we found that cDC1s are not solely required for Th1 responses, and the presence of these cDC1s can suppress excessive Th17 responses in BMT mice (**Figure 5B** and **C**). Potentially, the loss of cDC1s in *Batf3*$^{-/-}$ BMT mice increases the opportunities for cDC2s to interact with more naïve T cells. On the other hand, the cytokines released from cDC1s may inhibit the priming of Th17 by cDC2s. IL-2 secreted by cDC1s has been reported to mediate the suppression of Th17 responses in a mouse model of invasive pulmonary aspergillosis (71). We found that lung APCs isolated from infected BMT mice express significantly lower levels of *Il2* after re-stimulation with MHV-68 *ex vivo* than normal lung APCs do (**Figure S4A**). When supplementing the coculture of BMT APCs and CD4$^+$ T cells with 10 ng/ml of recombinant mouse IL-2, the expression of *Il17a* in CD4$^+$ T cells was significantly suppressed (**Figure S4B**). Similarly, supplementation of the coculture of BMT APCs and CD4$^+$ T cells with conditioned medium of non-BMT APCs also significantly suppressed the expression of *Il17a* (**Figure S4B**). Supplementation of IL-2 in the culture can also increase the expression of IFN-γ (**Figure S4C**). However, *in* vivo administration of IL-2 to BMT mice did not suppress Th17 differentiation

(**Figure S4 D** and **E**). Rather, due to the expansion of total $CD4^+$ and $CD8^+$ T cells stimulated by IL-2, the numbers of both Th17 and Th1 cells per lung were increased (**Figure D** to **F**). The administration of IL-2 also did not suppress viral replication in BMT mice (data not shown). Thus, further studies are warranted to determine how cDC1s might suppress Th17 in infected BMT mice in vivo.

Notably, the cDC2s prime Th17 responses against MHV-68 infection only in BMT mice, but not in non-BMT mice. Even in *Batf3*$^{-/-}$ non-BMT mice in which the suppression from cDC1s is lifted, Th17 response is still minimal after infection with MHV-68 (**Figure S2**). These data indicate that the microenvironmental conditions in BMT mice may have dictated cDC2s ability to promote Th17 responses to MHV-68. The production of IL-6 (72) and IL-23 (73) are essential for cDC2s to prime Th17 cells. The APCs isolated from BMT mice produce higher levels of IL-6 and IL-23 than normal APCs when stimulated with MHV-68 [**Figure 1C** and (24)]. DCs sense exogenous pathogens or tissue damage through pattern recognition receptors such as Toll-like receptors (TLRs) to stimulate NF-κB or other signaling pathways to upregulate inflammatory cytokines. The regulation of IL-6 expression and translation is fine-tuned at multiple levels [reviewed in (74)]. MHV-68 can be recognized by TLR2 and stimulate the expression of IL-6 (75). In addition, many bacterial, fungi and damage-associated molecular patterns can also bind to TLR2 or TLR9 and stimulate NF-κB leading to the expression of IL-6. BMT conditioning is associated with tissue damage and we have shown that the lung microbiome community structure and diversity is significantly shifted after MHV-68 infection in BMT mice (28), which we speculate may provide suitable conditions for stimulating cDC2s to become pro-Th17 APCs.

EBV and MHV-68 can cause splenomegaly in humans and mice, respectively. Mice develop a striking splenomegaly 2-3 weeks after infection with increased numbers of B cells and $CD4^+$ and $CD8^+$ T cells (76). The development of MHV-68-induced splenomegaly depends on $CD4^+$ T cells (76) and viral lytic replication in the B cells (77, 78). Infected DCs can pass the virus to B cells

(79). We found that mice with conditional knockout of *Notch2* in $CD11c^+$ cells do not develop splenomegaly (**Figure S1C** and **D**). Since lung cDC2s are required to induce T follicular helper cell (Tfh) differentiation in response to antigens (80) and support germinal center reactions (81), *Notch2*-dependent cDC2s are likely essential for both passing virus to B cells and subsequently stimulating germinal center reactions through Tfh cells. Note that MHV-68 infection can cause a considerable amount of B cells to express CD11c (82), and thus *Notch2* in these B cells is knocked out in our experimental system. Knock out of *Notch2* in these cells may also impair their proliferation and development in a similar manner as those seen in marginal zone or follicular B cells (83, 84).

In conclusion, our study identifies impaired cDC trafficking as the underlying cellular mechanism responsible for the reduced protective Th1 responses against MHV-68 infection in BMT mice. The priming of pathogenic Th17 responses which requires *Notch2* function in cDC2s can occur in the lung without cDC migration into the dLNs. Moreover, we revealed that the impaired cDC trafficking is not due to low expression levels of CCR7 on cDCs, but more likely due to defects in production of CCL21 in the lung, most likely in the lymphatic endothelial cells post-BMT. How the BMT procedure affects the lung cell production of CCL21 or other molecules critical for cDC migration in response to MHV-68 infection will be the focus of future studies. Collectively, our study provides new insights in the reason SCT recipients develop severe pulmonary consequences secondary to altered immune responses to viral infections.

Materials and Methods

Mice

C57BL/6 (B6), *Batf3*$^{-}$ (B6.129S(C)-Batf3^{tm1Kmm}/J), CD11c-Cre [B6.Cg-Tg(Itgax-cre)1–1Reiz/J], *Notch2*$^{f/f}$ (B6.129S-Notch2^{tm3Grid}/J), *Irf4*$^{f/f}$ (B6.129S1-Irf4^{tm1Rdf}/J), *CCR7*$^{-}$ (B6.129P2(C)-Ccr7^{tm1Rfor}/J) were acquired from Jackson Laboratories. *Notch2*$^{f/f}$ or *Irf4*$^{f/f}$ mice were crossed to CD11c-Cre mice to generate *Notch2*^{cKO} or *Irf4*^{cKO} mice. All mice were maintained on C57BL/6 background in a specific pathogen-free animal facility.

Syngeneic BMT and MHV-68 infection

Recipient B6 WT mice were treated with 13 Gy total body irradiation (split dose) using a ^{137}Cs irradiator, followed by tail vein injection of 5 x 10^6 whole bone marrow cells from WT, *Batf3*$^{-/-}$, *Notch2*^{cKO}, *Irf4*^{cKO}or *CCR7*$^{-/-}$ mice. Inoculation of MHV-68 was carried out at the fifth week after BMT, when total numbers of hematopoietic cells were fully reconstituted in the lungs and spleen (32). Non-BMT or BMT mice were infected with 5 x 10^4 pfu of murine MHV-68 (VR-1465, ATCC, Manassas, VA), intranasally after being anesthetized with ketamine and xylazine.

Cell preparation

Mice were euthanized with CO_2, and the lungs were perfused with 5 mL PBS delivered via the right ventricle of the heart before being isolated. The posterior mediastinal dLNs which the lung cDCs migrate into (85) were isolated. Single cell suspensions of leukocytes were prepared from whole lungs by collagenase digestion for flow cytometry as described previously (86). Briefly, each minced lung was incubated in 15 ml of complete media with 1 mg/ml collagenase (Boehringer Mannheim Biochemical, Chicago, IL), and 17 U/ml DNase I (Sigma-Aldrich, St. Louis, MO) for 30 minutes at 37°C. The digested tissue was drawn through the bore of a 10-ml syringe repeatedly, and filtered through 100 μm mesh.

Flow cytometry

To characterize T lymphocytes, lung or dLN single cells were stimulated with phorbol myristate acetate (PMA) (0.05 μg/ml; Sigma-Aldrich, St. Louis, MO) and ionomycin (0.75 μg/ml; Sigma-Aldrich, St. Louis, MO) for 4 h in the presence of GolgiStop protein transport inhibitor (BD Pharmingen, San Jose, CA) before antibody staining. An aliquot of 1 x 10^6 cells was first blocked by anti-CD16/CD32 (Fc block; BD Pharmingen, San Jose, CA) antibodies and then stained with fluorochrome-conjugated antibodies on ice against cell surface markers CD45 (clone 30-F11), CD90.2 (53-2.1), CD3 (145-2C11), CD4 (GK1.5), CD8 (53-6.7) and CD19 (1D3), all from BD Pharmingen. The cells were then permeabilized and fixed with Foxp3 staining buffer set (eBioscience) and stained for intracellular IL-17A (TC11-18H10) and IFN-γ (XMG1.2) from BD Pharmingen following the manufacturer's instructions. For characterization of lung APCs, lung or dLN single cells were stained with antibodies on ice specific for CD45 (clone 30-F11), CD11c (N418), CD103 (2E7), I-A^b (AF6-120.1), Siglec F (E50-2440), CD24 (M1/69) and CD68 (FA-11) from BioLegend, and CD11b (M1/70) from BD Pharmingen. Staining cell surface CCR7 were done by first incubating cells with anti-CCR7 (4B12, BD BioLegend) for 30 min at 37°C prior to additional surface staining on ice as above. Cells were analyzed on a LSRFortessa cell analyzer for flow cytometry (BD Biosciences).

Immunostaining of lung sections and microscopy

Immunofluorescence staining of frozen lung sections has been reported previously (24, 87). Briefly, frozen lung sections were fixed in 10% formalin, permeabilized by 0.1% Triton X-100, and followed by blocking with 1% bovine serum albumin in phosphate buffered saline. The lung sections were then incubated with primary antibodies overnight at 4°C followed by secondary antibodies for one hour at room temperature. Primary antibodies and dilutions used: rat anti-CD90.2/Thy-1.2 antibody (clone 30-H12, BD Biosciences Pharmingen, 1:300), goat anti-CCL21

(polyclonal, R&D Systems, 1:100) and Armenian hamster anti-CD11c conjugated with PE/Dazzle 594 (clone N418, Biolegend, 1:100). Secondary antibodies include donkey anti-rat Ig antibody conjugated with FITC (1:200) and donkey anti-goat Ig antibody conjugated with Alexa Fluor 647 (1:200) from Invitrogen. Images were collected on a Zeiss ApoTome fluorescent microscope using AxioVision software.

APCs and CD4+ T cells co-culture

APCs were enriched by $CD11c^+$ microbeads (Miltenyi Biotec) from lung single cell suspensions of BMT or non-BMT mice at 3 dpi. $CD4^+$ T cells were enriched by $CD4^+$ microbeads (Miltenyi Biotec) from BMT lung at 10 dpi. In a 48-well plate, 4×10^4 cell/well APCs were incubated with 0.125 multiplicity of infection (MOI) of MHV-68 for 3 hours before addition of 4×10^5 T cells. Cells were cultured in 0.5 ml RPMI 1640 medium supplemented with 10% FCS, 1% HEPES and 0.1% β-mercaptoethanol, or in conditioned medium collected from a 2-day culture of non-BMT lung APCs (4 parts of conditioned medium and one part of fresh medium) for 4 days. Where indicated, recombinant mouse IL-2 (PeproTech) was added to cultures to a final concentration of 10 ng/ml.

Quantitative RT-PCR

The relative amount of mRNA for viral genes or mouse genes was assayed by real-time RT-PCR using thermocycler ABI Prism 7000 (Applied Biosystems, Inc., Foster City, CA) using a previously described protocol (24). Mouse GAPDH was used as an internal control gene. Gene-specific primers and probes are detailed in Table 1.

Enzyme-linked immunosorbent assay (ELISA)

ELISA for IFN-γ or IL-17A was performed using R&D Systems kits according to manufacturer's instructions.

In Situ CFSE labelling

5μM CFSE (Invitrogen) was prepared by diluting a 50 μM CFSE stock in DMSO with PBS and then instilling 50 μl into each anesthetized mouse through oropharyngeal aspiration.

FTY720 or IL-2 treatment

Mice were injected intraperitoneally daily with 1 mg/kg FTY720 (Cayman Chemical) dissolved in sterile PBS between day 3 and 6 after infection with MHV-68. BMT mice received daily i.p. injections of recombinant murine IL-2 starting at 2 dpi with MHV-68 at a dose of 20,000 IU until 6 dpi. At 7 dpi, mice were euthanized for assays. Nontreated control mice received in equivalent volume of sterile PBS.

Statistics

When groups of 2 were compared, 2 tailed student's *t*-tests were used to determine significance; when groups of 3 or more were compared, one-way ANOVA was utilized with a Tukey's multiple comparisons test to determine significance.

Study approval

All murine experiments were performed according to NIH guidelines and approved by the Institutional Animal Care and Use Committee at the University of Michigan.

Author Contributions: X.Z. and B.B.M. designed the study; C.A.W., M.M.C., P.R.C., and X.Z. performed animal studies; C.A.W. and X.Z. analyzed data and wrote the initial manuscript; X.Z. and B.B.M. revised manuscript, and all other authors critically reviewed the manuscript drafts and approved the final version.

Acknowledgments: This work is supported by the post-doctoral translational scholar grant MICHR 2UL1TR000433 (X.Z.), HHV-6 Foundation Dharam Ablashi Research Fund Grant (X.Z.), and NIH grants HL144481 and AI117229 (B.B.M.). The authors thank the Unit for Laboratory Animal Medicine, the Experimental Irradiation Core and the Flow Cytometry Core Facility funded by P30CA046592 at the University of Michigan for technical support.

References:

1. Tomblyn M, Chiller T, Einsele H, Gress R, Sepkowitz K, Storek J, et al. Guidelines for preventing infectious complications among hematopoietic cell transplantation recipients: a global perspective. *Biology of blood and marrow transplantation : journal of the American Society for Blood and Marrow Transplantation.* 2009;15(10):1143-238.
2. Styczynski J, Czyzewski K, Wysocki M, Gryniewicz-Kwiatkowska O, Kolodziejczyk-Gietka A, Salamonowicz M, et al. Increased risk of infections and infection-related mortality in children undergoing haematopoietic stem cell transplantation compared to conventional anticancer therapy: a multicentre nationwide study. *Clinical microbiology and infection : the official publication of the European Society of Clinical Microbiology and Infectious Diseases.* 2016;22(2):179 e1- e10.
3. Wingard JR, Hsu J, and Hiemenz JW. Hematopoietic stem cell transplantation: an overview of infection risks and epidemiology. *Infectious disease clinics of North America.* 2010;24(2):257-72.
4. Admiraal R, de Koning CCH, Lindemans CA, Bierings MB, Wensing AMJ, Versluys AB, et al. Viral reactivations and associated outcomes in the context of immune reconstitution after pediatric hematopoietic cell transplantation. *J Allergy Clin Immunol.* 2017;140(6):1643-50 e9.
5. Fedele R, Martino M, Garreffa C, Messina G, Console G, Princi D, et al. The impact of early CD4+ lymphocyte recovery on the outcome of patients who undergo allogeneic bone marrow or peripheral blood stem cell transplantation. *Blood Transfus.* 2012;10(2):174-80.
6. Kim DH, Sohn SK, Won DI, Lee NY, Suh JS, and Lee KB. Rapid helper T-cell recovery above 200 x 10 6/l at 3 months correlates to successful transplant outcomes after allogeneic stem cell transplantation. *Bone marrow transplantation.* 2006;37(12):1119-28.
7. Ritter J, Seitz V, Balzer H, Gary R, Lenze D, Moi S, et al. Donor CD4 T Cell Diversity Determines Virus Reactivation in Patients After HLA-Matched Allogeneic Stem Cell Transplantation. *Am J Transplant.* 2015;15(8):2170-9.
8. Storek J, Gooley T, Witherspoon RP, Sullivan KM, and Storb R. Infectious morbidity in long-term survivors of allogeneic marrow transplantation is associated with low CD4 T cell counts. *Am J Hematol.* 1997;54(2):131-8.
9. Storek J, Geddes M, Khan F, Huard B, Helg C, Chalandon Y, et al. Reconstitution of the immune system after hematopoietic stem cell transplantation in humans. *Seminars in immunopathology.* 2008;30(4):425-37.
10. Martin PJ, Counts GW, Jr., Appelbaum FR, Lee SJ, Sanders JE, Deeg HJ, et al. Life expectancy in patients surviving more than 5 years after hematopoietic cell transplantation. *Journal of clinical oncology : official journal of the American Society of Clinical Oncology.* 2010;28(6):1011-6.
11. Abou-Mourad YR, Lau BC, Barnett MJ, Forrest DL, Hogge DE, Nantel SH, et al. Long-term outcome after allo-SCT: close follow-up on a large cohort treated with myeloablative regimens. *Bone marrow transplantation.* 2010;45(2):295-302.
12. Wingard JR, Majhail NS, Brazauskas R, Wang Z, Sobocinski KA, Jacobsohn D, et al. Long-term survival and late deaths after allogeneic hematopoietic cell transplantation. *Journal of clinical oncology : official journal of the American Society of Clinical Oncology.* 2011;29(16):2230-9.
13. Norkin M, Shaw BE, Brazauskas R, Tecca HR, Leather HL, Gea-Banacloche J, et al. Characteristics of Late Fatal Infections after Allogeneic Hematopoietic Cell Transplantation. *Biology of blood and marrow transplantation : journal of the American Society for Blood and Marrow Transplantation.* 2019;25(2):362-8.

14. Jantunen E, Itala M, Siitonen T, Koivunen E, Leppa S, Juvonen E, et al. Late non-relapse mortality among adult autologous stem cell transplant recipients: a nation-wide analysis of 1,482 patients transplanted in 1990-2003. *Eur J Haematol.* 2006;77(2):114-9.
15. Antin JH, and Ferrara JL. Cytokine dysregulation and acute graft-versus-host disease. *Blood.* 1992;80(12):2964-8.
16. Chklovskaia E, Nowbakht P, Nissen C, Gratwohl A, Bargetzi M, and Wodnar-Filipowicz A. Reconstitution of dendritic and natural killer-cell subsets after allogeneic stem cell transplantation: effects of endogenous flt3 ligand. *Blood.* 2004;103(10):3860-8.
17. DiCarlo J, Agarwal-Hashmi R, Shah A, Kim P, Craveiro L, Killen R, et al. Cytokine and chemokine patterns across 100 days after hematopoietic stem cell transplantation in children. *Biology of blood and marrow transplantation : journal of the American Society for Blood and Marrow Transplantation.* 2014;20(3):361-9.
18. Henden AS, and Hill GR. Cytokines in Graft-versus-Host Disease. *Journal of immunology.* 2015;194(10):4604-12.
19. Kelly RM, Goren EM, Taylor PA, Mueller SN, Stefanski HE, Osborn MJ, et al. Short-term inhibition of p53 combined with keratinocyte growth factor improves thymic epithelial cell recovery and enhances T-cell reconstitution after murine bone marrow transplantation. *Blood.* 2010;115(5):1088-97.
20. Kelly RM, Highfill SL, Panoskaltsis-Mortari A, Taylor PA, Boyd RL, Hollander GA, et al. Keratinocyte growth factor and androgen blockade work in concert to protect against conditioning regimen-induced thymic epithelial damage and enhance T-cell reconstitution after murine bone marrow transplantation. *Blood.* 2008;111(12):5734-44.
21. Stefanski HE, Jonart L, Goren E, Mule JJ, and Blazar BR. A novel approach to improve immune effector responses post transplant by restoration of CCL21 expression. *PLoS One.* 2018;13(4):e0193461.
22. Stein JV, Rot A, Luo Y, Narasimhaswamy M, Nakano H, Gunn MD, et al. The CC chemokine thymus-derived chemotactic agent 4 (TCA-4, secondary lymphoid tissue chemokine, 6Ckine, exodus-2) triggers lymphocyte function-associated antigen 1-mediated arrest of rolling T lymphocytes in peripheral lymph node high endothelial venules. *The Journal of experimental medicine.* 2000;191(1):61-76.
23. Braun A, Worbs T, Moschovakis GL, Halle S, Hoffmann K, Bolter J, et al. Afferent lymph-derived T cells and DCs use different chemokine receptor CCR7-dependent routes for entry into the lymph node and intranodal migration. *Nat Immunol.* 2011;12(9):879-87.
24. Zhou X, Loomis-King H, Gurczynski SJ, Wilke CA, Konopka KE, Ptaschinski C, et al. Bone marrow transplantation alters lung antigen-presenting cells to promote TH17 response and the development of pneumonitis and fibrosis following gammaherpesvirus infection. *Mucosal Immunol.* 2016;9(3):610-20.
25. Reid GE, Lynch JP, 3rd, Weigt S, Sayah D, Belperio JA, Grim SA, et al. Herpesvirus Respiratory Infections in Immunocompromised Patients: Epidemiology, Management, and Outcomes. *Semin Respir Crit Care Med.* 2016;37(4):603-30.
26. Boeckh M, Leisenring W, Riddell SR, Bowden RA, Huang ML, Myerson D, et al. Late cytomegalovirus disease and mortality in recipients of allogeneic hematopoietic stem cell transplants: importance of viral load and T-cell immunity. *Blood.* 2003;101(2):407-14.
27. Seo S, Renaud C, Kuypers JM, Chiu CY, Huang ML, Samayoa E, et al. Idiopathic pneumonia syndrome after hematopoietic cell transplantation: evidence of occult infectious etiologies. *Blood.* 2015;125(24):3789-97.

28. O'Dwyer DN, Zhou X, Wilke CA, Xia M, Falkowski NR, Norman KC, et al. Lung Dysbiosis, Inflammation, and Injury in Hematopoietic Cell Transplantation. *Am J Respir Crit Care Med.* 2018.
29. Versluys AB, Rossen JW, van Ewijk B, Schuurman R, Bierings MB, and Boelens JJ. Strong association between respiratory viral infection early after hematopoietic stem cell transplantation and the development of life-threatening acute and chronic alloimmune lung syndromes. *Biology of blood and marrow transplantation : journal of the American Society for Blood and Marrow Transplantation.* 2010;16(6):782-91.
30. Zhou X, O'Dwyer DN, Xia M, Miller HK, Chan PR, Trulik K, et al. First Onset Herpesviral Infection and Lung Injury in Allogeneic Hematopoietic Cell Transplantation. *Am J Respir Crit Care Med.* 2019.
31. Auletta JJ, Devecchio JL, Ferrara JL, and Heinzel FP. Distinct phases in recovery of reconstituted innate cellular-mediated immunity after murine syngeneic bone marrow transplantation. *Biology of blood and marrow transplantation : journal of the American Society for Blood and Marrow Transplantation.* 2004;10(12):834-47.
32. Hubbard LL, Ballinger MN, Wilke CA, and Moore BB. Comparison of conditioning regimens for alveolar macrophage reconstitution and innate immune function post bone marrow transplant. *Exp Lung Res.* 2008;34(5):263-75.
33. Coomes SM, Hubbard LL, and Moore BB. Impaired pulmonary immunity post-bone marrow transplant. *Immunologic research.* 2011;50(1):78-86.
34. Coomes SM, Farmen S, Wilke CA, Laouar Y, and Moore BB. Severe gammaherpesvirus-induced pneumonitis and fibrosis in syngeneic bone marrow transplant mice is related to effects of transforming growth factor-beta. *The American journal of pathology.* 2011;179(5):2382-96.
35. Gurczynski SJ, Zhou X, Flaherty M, Wilke CA, and Moore BB. Bone marrow transplant-induced alterations in Notch signaling promote pathologic Th17 responses to gamma-herpesvirus infection. *Mucosal Immunol.* 2018;11(3):881-93.
36. Kopf M, Schneider C, and Nobs SP. The development and function of lung-resident macrophages and dendritic cells. *Nat Immunol.* 2015;16(1):36-44.
37. Worbs T, Hammerschmidt SI, and Forster R. Dendritic cell migration in health and disease. *Nat Rev Immunol.* 2017;17(1):30-48.
38. Guilliams M, Ginhoux F, Jakubzick C, Naik SH, Onai N, Schraml BU, et al. Dendritic cells, monocytes and macrophages: a unified nomenclature based on ontogeny. *Nat Rev Immunol.* 2014;14(8):571-8.
39. Murphy TL, Grajales-Reyes GE, Wu X, Tussiwand R, Briseno CG, Iwata A, et al. Transcriptional Control of Dendritic Cell Development. *Annu Rev Immunol.* 2016;34:93-119.
40. Langlet C, Tamoutounour S, Henri S, Luche H, Ardouin L, Gregoire C, et al. CD64 expression distinguishes monocyte-derived and conventional dendritic cells and reveals their distinct role during intramuscular immunization. *Journal of immunology.* 2012;188(4):1751-60.
41. Plantinga M, Guilliams M, Vanheerswynghels M, Deswarte K, Branco-Madeira F, Toussaint W, et al. Conventional and monocyte-derived CD11b(+) dendritic cells initiate and maintain T helper 2 cell-mediated immunity to house dust mite allergen. *Immunity.* 2013;38(2):322-35.
42. Guilliams M, De Kleer I, Henri S, Post S, Vanhoutte L, De Prijck S, et al. Alveolar macrophages develop from fetal monocytes that differentiate into long-lived cells in the first week of life via GM-CSF. *The Journal of experimental medicine.* 2013;210(10):1977-92.
43. Weber M, Hauschild R, Schwarz J, Moussion C, de Vries I, Legler DF, et al. Interstitial dendritic cell guidance by haptotactic chemokine gradients. *Science.* 2013;339(6117):328-32.

44. Lo JC, Chin RK, Lee Y, Kang HS, Wang Y, Weinstock JV, et al. Differential regulation of CCL21 in lymphoid/nonlymphoid tissues for effectively attracting T cells to peripheral tissues. *J Clin Invest.* 2003;112(10):1495-505.
45. Schumann K, Lammermann T, Bruckner M, Legler DF, Polleux J, Spatz JP, et al. Immobilized chemokine fields and soluble chemokine gradients cooperatively shape migration patterns of dendritic cells. *Immunity.* 2010;32(5):703-13.
46. Kretschmer S, Dethlefsen I, Hagner-Benes S, Marsh LM, Garn H, and Konig P. Visualization of intrapulmonary lymph vessels in healthy and inflamed murine lung using CD90/Thy-1 as a marker. *PLoS One.* 2013;8(2):e55201.
47. Permanyer M, Bosnjak B, and Forster R. Dendritic cells, T cells and lymphatics: dialogues in migration and beyond. *Current opinion in immunology.* 2018;53:173-9.
48. Hildner K, Edelson BT, Purtha WE, Diamond M, Matsushita H, Kohyama M, et al. Batf3 deficiency reveals a critical role for CD8alpha+ dendritic cells in cytotoxic T cell immunity. *Science.* 2008;322(5904):1097-100.
49. Torti N, Walton SM, Murphy KM, and Oxenius A. Batf3 transcription factor-dependent DC subsets in murine CMV infection: differential impact on T-cell priming and memory inflation. *European journal of immunology.* 2011;41(9):2612-8.
50. Lewis KL, Caton ML, Bogunovic M, Greter M, Grajkowska LT, Ng D, et al. Notch2 receptor signaling controls functional differentiation of dendritic cells in the spleen and intestine. *Immunity.* 2011;35(5):780-91.
51. Satpathy AT, Briseno CG, Lee JS, Ng D, Manieri NA, Kc W, et al. Notch2-dependent classical dendritic cells orchestrate intestinal immunity to attaching-and-effacing bacterial pathogens. *Nat Immunol.* 2013;14(9):937-48.
52. Schlitzer A, McGovern N, Teo P, Zelante T, Atarashi K, Low D, et al. IRF4 transcription factor-dependent CD11b+ dendritic cells in human and mouse control mucosal IL-17 cytokine responses. *Immunity.* 2013;38(5):970-83.
53. Williams JW, Tjota MY, Clay BS, Vander Lugt B, Bandukwala HS, Hrusch CL, et al. Transcription factor IRF4 drives dendritic cells to promote Th2 differentiation. *Nat Commun.* 2013;4:2990.
54. Bajana S, Turner S, Paul J, Ainsua-Enrich E, and Kovats S. IRF4 and IRF8 Act in CD11c+ Cells To Regulate Terminal Differentiation of Lung Tissue Dendritic Cells. *Journal of immunology.* 2016;196(4):1666-77.
55. Chiba K, Yanagawa Y, Masubuchi Y, Kataoka H, Kawaguchi T, Ohtsuki M, et al. FTY720, a novel immunosuppressant, induces sequestration of circulating mature lymphocytes by acceleration of lymphocyte homing in rats. I. FTY720 selectively decreases the number of circulating mature lymphocytes by acceleration of lymphocyte homing. *Journal of immunology.* 1998;160(10):5037-44.
56. Pham TH, Baluk P, Xu Y, Grigorova I, Bankovich AJ, Pappu R, et al. Lymphatic endothelial cell sphingosine kinase activity is required for lymphocyte egress and lymphatic patterning. *The Journal of experimental medicine.* 2010;207(1):17-27.
57. Caucheteux SM, Torabi-Parizi P, and Paul WE. Analysis of naive lung CD4 T cells provides evidence of functional lung to lymph node migration. *Proc Natl Acad Sci U S A.* 2013;110(5):1821-6.
58. Lan YY, De Creus A, Colvin BL, Abe M, Brinkmann V, Coates PT, et al. The sphingosine-1-phosphate receptor agonist FTY720 modulates dendritic cell trafficking in vivo. *Am J Transplant.* 2005;5(11):2649-59.
59. Russo E, Teijeira A, Vaahtomeri K, Willrodt AH, Bloch JS, Nitschke M, et al. Intralymphatic CCL21 Promotes Tissue Egress of Dendritic Cells through Afferent Lymphatic Vessels. *Cell Rep.* 2016;14(7):1723-34.

60. Tal O, Lim HY, Gurevich I, Milo I, Shipony Z, Ng LG, et al. DC mobilization from the skin requires docking to immobilized CCL21 on lymphatic endothelium and intralymphatic crawling. *The Journal of experimental medicine.* 2011;208(10):2141-53.
61. Ulvmar MH, Werth K, Braun A, Kelay P, Hub E, Eller K, et al. The atypical chemokine receptor CCRL1 shapes functional CCL21 gradients in lymph nodes. *Nat Immunol.* 2014;15(7):623-30.
62. Chung J, Ebens CL, Perkey E, Radojcic V, Koch U, Scarpellino L, et al. Fibroblastic niches prime T cell alloimmunity through Delta-like Notch ligands. *J Clin Invest.* 2017;127(4):1574-88.
63. Mueller SN, Hosiawa-Meagher KA, Konieczny BT, Sullivan BM, Bachmann MF, Locksley RM, et al. Regulation of homeostatic chemokine expression and cell trafficking during immune responses. *Science (New York, N Y).* 2007;317(5838):670-4.
64. Curtis J, Luo Y, Zenner HL, Cuchet-Lourenco D, Wu C, Lo K, et al. Susceptibility to tuberculosis is associated with variants in the ASAP1 gene encoding a regulator of dendritic cell migration. *Nature genetics.* 2015;47(5):523-7.
65. Vassallo R, Walters PR, Lamont J, Kottom TJ, Yi ES, and Limper AH. Cigarette smoke promotes dendritic cell accumulation in COPD; a Lung Tissue Research Consortium study. *Respiratory research.* 2010;11:45.
66. Demedts IK, Bracke KR, Van Pottelberge G, Testelmans D, Verleden GM, Vermassen FE, et al. Accumulation of dendritic cells and increased CCL20 levels in the airways of patients with chronic obstructive pulmonary disease. *Am J Respir Crit Care Med.* 2007;175(10):998-1005.
67. Finch DK, Stolberg VR, Ferguson J, Alikaj H, Kady MR, Richmond BW, et al. Lung Dendritic Cells Drive Natural Killer Cytotoxicity in Chronic Obstructive Pulmonary Disease via IL-15Ralpha. *Am J Respir Crit Care Med.* 2018;198(9):1140-50.
68. Arellano-Orden E, Calero-Acuna C, Moreno-Mata N, Gomez-Izquierdo L, Sanchez-Lopez V, Lopez-Ramirez C, et al. Cigarette Smoke Decreases the Maturation of Lung Myeloid Dendritic Cells. *PLoS One.* 2016;11(4):e0152737.
69. Tussiwand R, Everts B, Grajales-Reyes GE, Kretzer NM, Iwata A, Bagaitkar J, et al. Klf4 expression in conventional dendritic cells is required for T helper 2 cell responses. *Immunity.* 2015;42(5):916-28.
70. Furuhashi K, Suda T, Hasegawa H, Suzuki Y, Hashimoto D, Enomoto N, et al. Mouse lung CD103+ and CD11bhigh dendritic cells preferentially induce distinct CD4+ T-cell responses. *Am J Respir Cell Mol Biol.* 2012;46(2):165-72.
71. Zelante T, Wong AY, Ping TJ, Chen J, Sumatoh HR, Vigano E, et al. CD103(+) Dendritic Cells Control Th17 Cell Function in the Lung. *Cell Rep.* 2015;12(11):1789-801.
72. Heink S, Yogev N, Garbers C, Herwerth M, Aly L, Gasperi C, et al. Trans-presentation of IL-6 by dendritic cells is required for the priming of pathogenic TH17 cells. *Nature immunology.* 2017;18(1):74-85.
73. Gelderblom M, Gallizioli M, Ludewig P, Thom V, Arunachalam P, Rissiek B, et al. IL-23 (Interleukin-23)-Producing Conventional Dendritic Cells Control the Detrimental IL-17 (Interleukin-17) Response in Stroke. *Stroke.* 2018;49(1):155-64.
74. Tanaka T, Narazaki M, and Kishimoto T. IL-6 in inflammation, immunity, and disease. *Cold Spring Harb Perspect Biol.* 2014;6(10):a016295.
75. Michaud F, Coulombe F, Gaudreault E, Kriz J, and Gosselin J. Involvement of TLR2 in recognition of acute gammaherpesvirus-68 infection. *PLoS One.* 2010;5(10):e13742.
76. Usherwood EJ, Ross AJ, Allen DJ, and Nash AA. Murine gammaherpesvirus-induced splenomegaly: a critical role for CD4 T cells. *J Gen Virol.* 1996;77 (Pt 4):627-30.
77. Usherwood EJ, Stewart JP, Robertson K, Allen DJ, and Nash AA. Absence of splenic latency in murine gammaherpesvirus 68-infected B cell-deficient mice. *J Gen Virol.* 1996;77 (Pt 11):2819-25.

78. Lawler C, de Miranda MP, May J, Wyer O, Simas JP, and Stevenson PG. Gammaherpesvirus Colonization of the Spleen Requires Lytic Replication in B Cells. *Journal of virology.* 2018;92(7).
79. Gaspar M, May JS, Sukla S, Frederico B, Gill MB, Smith CM, et al. Murid herpesvirus-4 exploits dendritic cells to infect B cells. *PLoS Pathog.* 2011;7(11):e1002346.
80. Krishnaswamy JK, Gowthaman U, Zhang B, Mattsson J, Szeponik L, Liu D, et al. Migratory CD11b(+) conventional dendritic cells induce T follicular helper cell-dependent antibody responses. *Sci Immunol.* 2017;2(18).
81. Briseno CG, Satpathy AT, Davidson JTt, Ferris ST, Durai V, Bagadia P, et al. Notch2-dependent DC2s mediate splenic germinal center responses. *Proc Natl Acad Sci U S A.* 2018;115(42):10726-31.
82. Rubtsova K, Rubtsov AV, van Dyk LF, Kappler JW, and Marrack P. T-box transcription factor T-bet, a key player in a unique type of B-cell activation essential for effective viral clearance. *Proc Natl Acad Sci U S A.* 2013;110(34):E3216-24.
83. Thomas M, Calamito M, Srivastava B, Maillard I, Pear WS, and Allman D. Notch activity synergizes with B-cell-receptor and CD40 signaling to enhance B-cell activation. *Blood.* 2007;109(8):3342-50.
84. Saito T, Chiba S, Ichikawa M, Kunisato A, Asai T, Shimizu K, et al. Notch2 is preferentially expressed in mature B cells and indispensable for marginal zone B lineage development. *Immunity.* 2003;18(5):675-85.
85. Ho AW, Prabhu N, Betts RJ, Ge MQ, Dai X, Hutchinson PE, et al. Lung CD103+ dendritic cells efficiently transport influenza virus to the lymph node and load viral antigen onto MHC class I for presentation to CD8 T cells. *Journal of immunology.* 2011;187(11):6011-21.
86. Coomes SM, Wilke CA, Moore TA, and Moore BB. Induction of TGF-beta 1, not regulatory T cells, impairs antiviral immunity in the lung following bone marrow transplant. *Journal of immunology.* 2010;184(9):5130-40.
87. Zhou X, and Moore BB. Lung Section Staining and Microscopy. *Bio Protoc.* 2017;7(10).
88. Sagi Y, Heiman M, Peterson JD, Musatov S, Scarduzio M, Logan SM, et al. Nitric oxide regulates synaptic transmission between spiny projection neurons. *Proc Natl Acad Sci U S A.* 2014;111(49):17636-41.
89. Ikeda T, Kajita K, Zhiliang W, Hanamoto T, Mori I, Fujioka K, et al. Effects of phorbol ester-sensitive PKC (c/nPKC) activation on the production of adiponectin in 3T3-L1 adipocytes. *IUBMB life.* 2009;61(6):644-50.
90. Chen SC, Vassileva G, Kinsley D, Holzmann S, Manfra D, Wiekowski MT, et al. Ectopic expression of the murine chemokines CCL21a and CCL21b induces the formation of lymph node-like structures in pancreas, but not skin, of transgenic mice. *Journal of immunology.* 2002;168(3):1001-8.
91. Luther SA, Tang HL, Hyman PL, Farr AG, and Cyster JG. Coexpression of the chemokines ELC and SLC by T zone stromal cells and deletion of the ELC gene in the plt/plt mouse. *Proc Natl Acad Sci U S A.* 2000;97(23):12694-9.

Figure 1

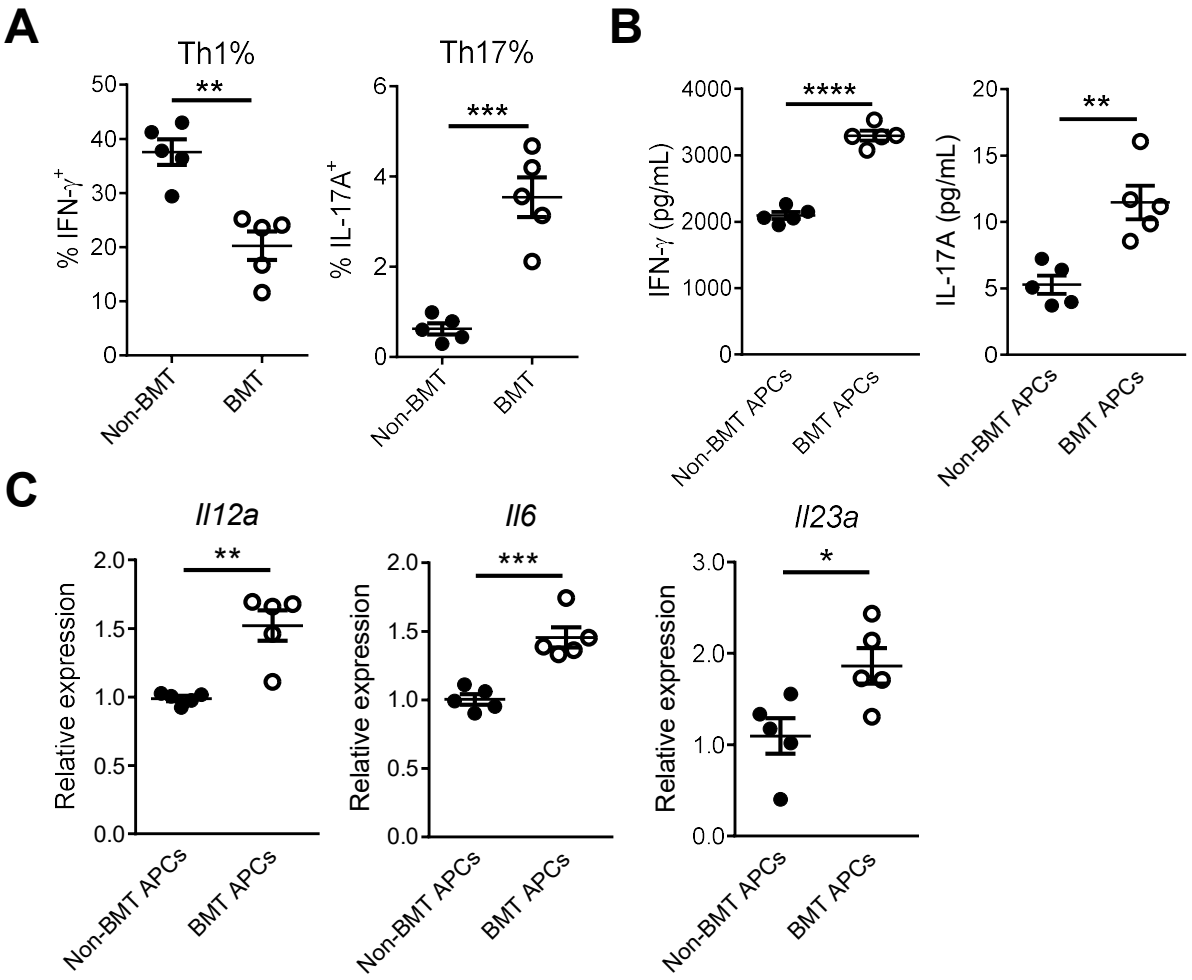

Figure 1. APCs from lungs of BMT mice are potent in priming both Th1 and Th17 responses *in vitro*. **(A)** Single cell suspensions were prepared by collagenase digestion of whole lungs of non-BMT (n=5) or BMT (n=5) mice at 7 dpi with MHV-68. Cells were then stimulated with PMA and ionomycin for 4 hours before antibody staining. Percent of $CD4^+$ T cells (*i.e.* $CD45^+CD90.2^+CD3^+CD4^+$) that express IFN-γ (Th1 cells), and percent of $CD4^+$ T cells that express IL-17A (Th17 cells) were determined by flow cytometry. **(B** and **C)** APCs enriched by $CD11c^+$ microbeads and pooled from lung single cell suspensions of 5 BMT or non-BMT mice at 3 dpi were co-cultured with pooled $CD4^+$ T cells from 10 BMT mice lungs at 10 dpi at a 1:10 ratio in the presence of 0.125 MOI of MHV-68 (n=5, each). **(B)** The concentration of IFN-γ or IL-17A in the supernatant of co-culture at 4 days was determined by ELISA (Mean + SEM, n = 5). **(C)** Co-cultured cells were pelleted at 4 days post co-culture and total RNA was isolated by Trizol. The expression of a pro-Th1 cytokine (*IL12A*) or pro-Th17 cytokines (*IL6* and *IL23A*) were determined by real time RT-PCR (Mean + SEM, n = 5). Symbols represent individual data points from unique mice. * $P < 0.05$, ** $P < 0.01$, *** $P < 0.001$, **** $P < 0.0001$, Student's *t*-test (2 tailed). Similar results were obtained in two additional experiments. APCs, antigen-presenting cells; BMT, bone marrow transplantation.

Figure 2

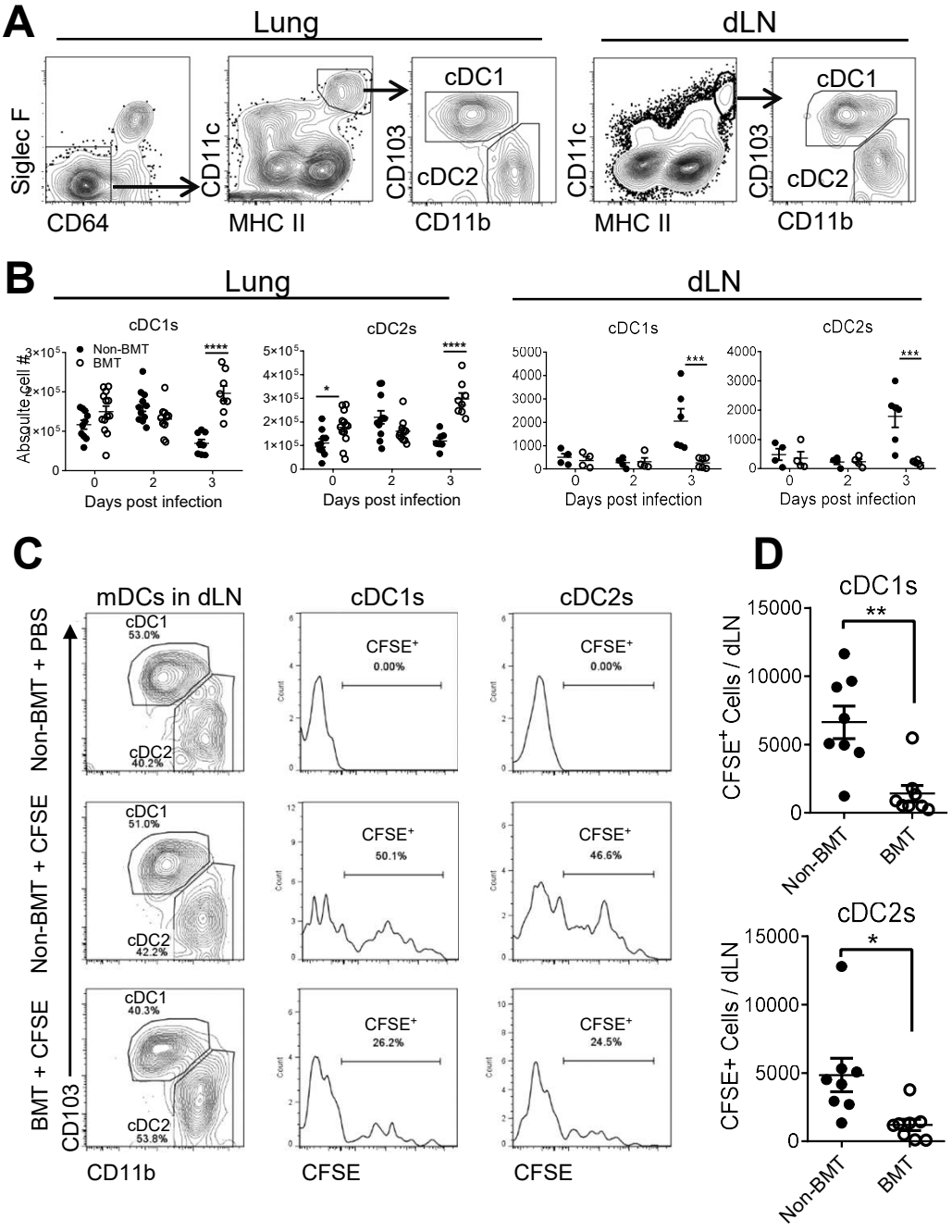
A
Lung
dLN
Siglec F
CD64
CD11c
MHC II
cDC1
cDC2
CD103
CD11b
B
Lung
dLN
cDC1s
cDC2s
Non-BMT
BMT
Absolute cell #
Days post infection
C
mDCs in dLN
cDC1s
cDC2s
Non-BMT + PBS
Non-BMT + CFSE
BMT + CFSE
CD103
CD11b
CFSE
CFSE+
0.00%
50.1%
46.6%
26.2%
24.5%
53.0%
40.2%
51.0%
42.2%
40.3%
53.8%
D
cDC1s
cDC2s
CFSE+ Cells / dLN
Non-BMT
BMT

Figure 2. Impaired migration of cDCs from the lung to dLN in BMT mice determined by the kinetics of cDC subsets in the lung and dLN or tracking CFSE-labeled lung cDCs. **(A)** Gating strategy. Lung or dLN single cell suspensions were prepared from mice at 3 dpi. Doublet-cell excluded live lung cells were plotted as Siglec F versus CD64 to exclude Siglec F^+ and/or $CD64^+$ macrophages and monocyte-derived cells. Among the remaining lung cells, cDCs were identified as a $CD11c^{hi}MHCII^{hi}$ population which can be further differentiated as cDC1s and cDC2s based on their expression of CD103 and CD11b. Similarly, migratory cDCs in dLN were identified as a $CD11c^+MHCII^{hi}$ population with cDC1 and cDC2 subsets. **(B)** Kinetics of cDC1s and cDC2s in the lungs or dLN of non-BMT or BMT mice at 0, 2 or 3 dpi (n=8~13, lung; n=4~6, dLN). The absolute numbers of cDC1s or cDC2s per lung or dLN were calculated by multiplying the total cell number of the organ with the percentage of the cell type determined by flow cytometry (Mean ± SEM). Symbols represent individual data points. *** $P < 0.001$, **** $P < 0.0001$, Student's *t*-test (2 tailed) between non-BMT and BMT mice. Similar results were obtained in two additional experiments. **(C** and **D)** Two days after viral infection, non-BMT or BMT mice were instilled with CFSE dye via oropharyngeal aspiration. Lung dLNs were harvested at 18 hrs post CFSE instillation. Single-cell suspensions were prepared for antibody staining and flow cytometric analysis. **(C)** Live single dLN cells were pre-gated for mDCs as in Fig. 2A, and two-color histograms for CD103 and CD11b expression were analyzed for cDC1 and cDC2 subsets. Numbers indicate the percent of cells in the gate. Single-color histograms determined the percent of $CFSE^+$ cells in each cDC subset. **(D)** Absolute numbers of $CFSE^+$ cells of each cDC subset per dLN of non-BMT (n=8) or BMT (n=8) mice, calculated by multiplying the total cell number of a dLN with the percentage of $CFSE^+$ cells (Mean ± SEM). Symbols represent individual mouse data points. Data were pooled from two independent experiments. * $P < 0.05$, ** $P < 0.01$, Student's *t*-test (2 tailed). BMT, bone marrow transplantation; cDC1, type 1 conventional dendritic cell; cDC2, type 2 conventional dendritic cell; dLN, draining lymph node; mDC, migratory dendritic cell.

Figure 3

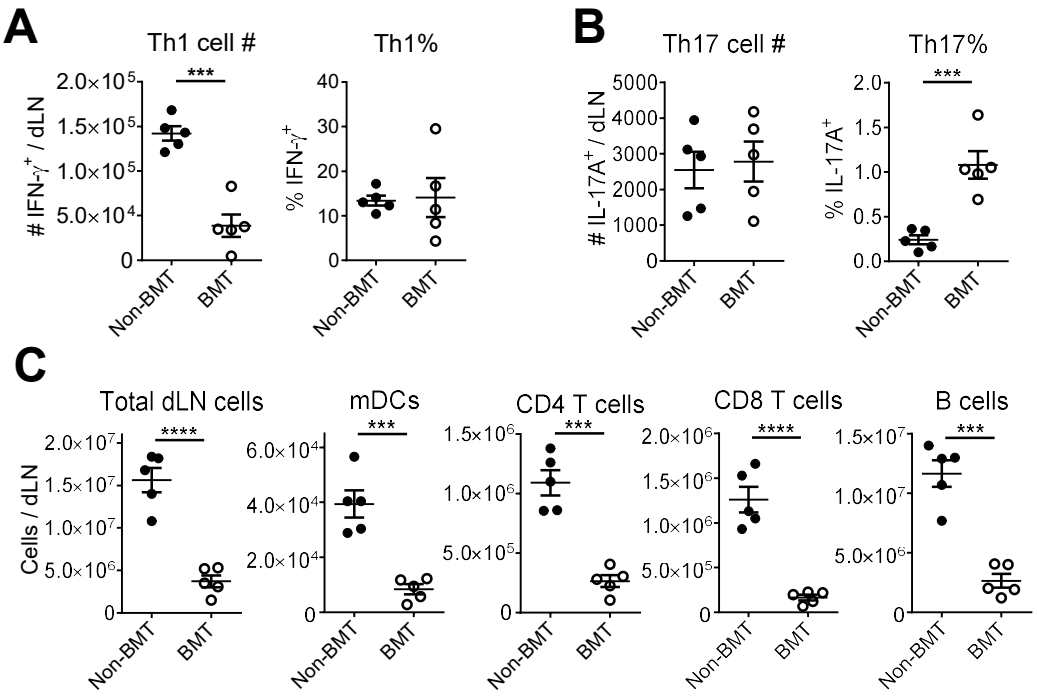

Figure 3. Th cell differentiation and cellularity in dLNs are correlated with DC migration phenotypes in non-BMT or BMT mice. (A) Absolute numbers IFN-γ^+ Th1 cells per dLN and percent of Th1 cells among $CD4^+$ T cells (pregated for $CD45^+CD90.2^+CD3^+CD4^+$). **(B)** Absolute numbers of IL-$17A^+$ Th17 cells per dLN and percent of Th17 cells among $CD4^+$ T cells. **(C)** Total cell numbers of dLNs of non-BMT or BMT mice at 7 dpi with MHV-68 were determined by hemocytometer counting. The absolute numbers of mDCs, $CD4^+$ Th, $CD8^+$ T and B cells per dLN were determined by total dLN cell numbers and percentage of flow cytometry based on cell surface markers. Mean ± SEM is shown for all panels and n=5 for each group. Similar results were obtained in two additional experiments. Symbols represent individual mouse data points. *** $P < 0.001$, **** $P < 0.0001$, Student's *t*-test (2 tailed). BMT, bone marrow transplantation; dLN, draining lymph node; mDC, migratory dendritic cell.

Figure 4

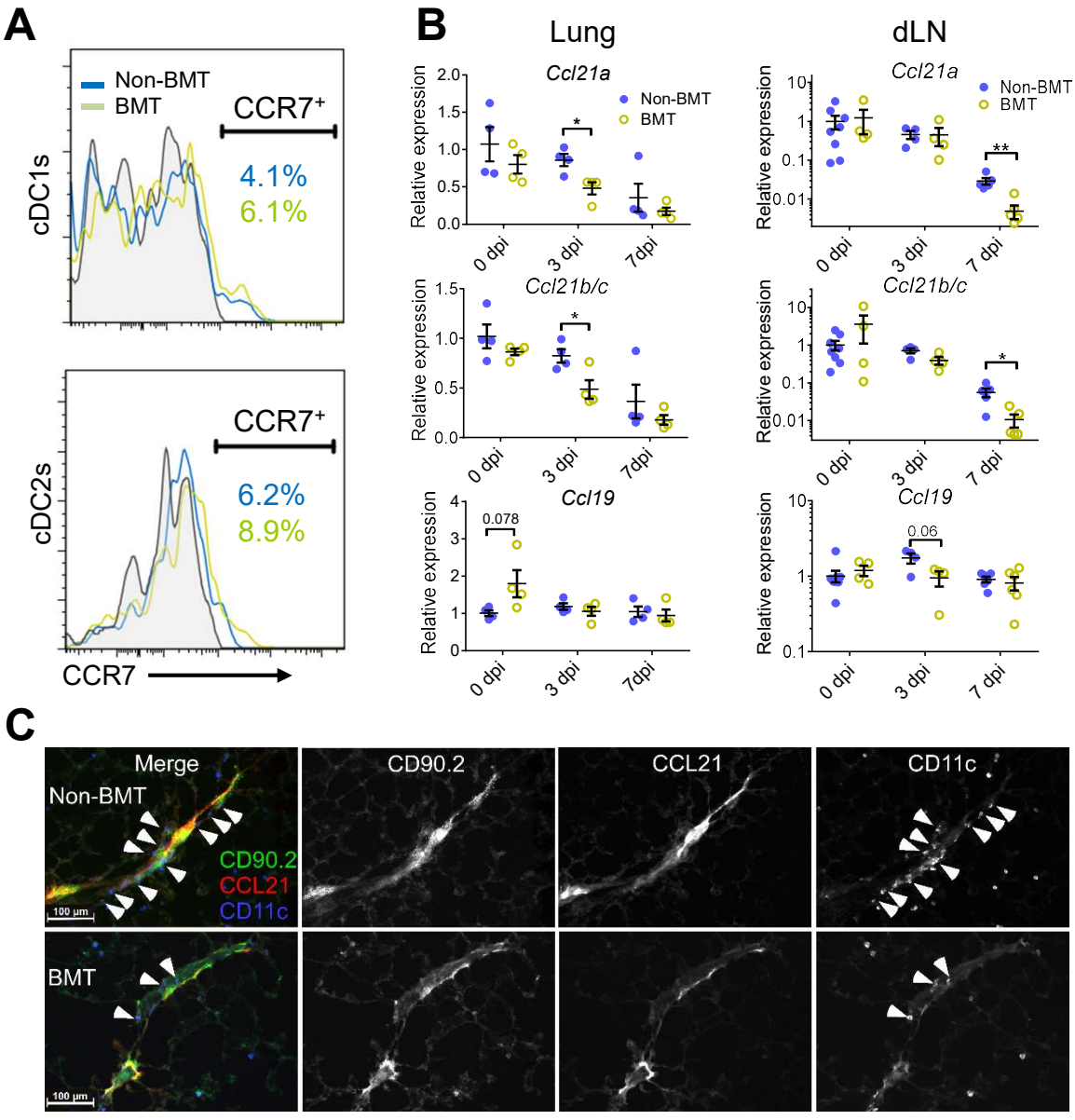
A
Non-BMT
BMT
CCR7+
cDC1s
4.1%
6.1%
CCR7+
cDC2s
6.2%
8.9%
CCR7
B
Lung
dLN
Ccl21a
Ccl21b/c
Ccl19
Relative expression
Non-BMT
BMT
0 dpi
3 dpi
7dpi
7 dpi
0.078
0.06
C
Merge
Non-BMT
CD90.2
CCL21
CD11c
100 μm
BMT

Figure 4. The expression of chemokine *Ccl21* in the lung is reduced in BMT mice but the expression of CCR7 on cDCs is not affected by BMT. **(A)** Representative single-color histograms determined the percentage of $CCR7^+$ cells in each cDC subset at 2 dpi. Gray areas represent the fluorescence minus one (FMO) control. Numbers indicate the percent of cells in the gate. Similar results were obtained in two additional experiments. **(B)** Relative mRNA abundance of *Ccl21a, Ccl21b/c* and *Ccl19* in dLNs and lung tissues of non-BMT or BMT mice at 0, 3 or 7 dpi (n=4~8, Mean ± SEM). Symbols represent individual mouse data points. * $P < 0.05$, ** $P < 0.01$, Student's *t*-test (2 tailed). **(C)** Multiple-color immunofluorescence staining of lung frozen sections prepared at 3dpi. Labelling of CD90.2 protein (green) identifies lymph vessels in the lung. Labelling of CCL21 protein (red) is co-localized with CD90.2. CD11c (blue) labels DCs and alveolar macrophages. There are numerous $CD11c^+$ cells within or in contact with lymph vessels (arrowheads) in non-BMT lungs but fewer such cells in the BMT lungs. Images represent two to three mice per group and two independent experiments. Bar=100 μm. BMT, bone marrow transplantation; cDC1, type 1 conventional dendritic cell; cDC2, type 2 conventional dendritic cell; dLN, draining lymph node.

Figure 5

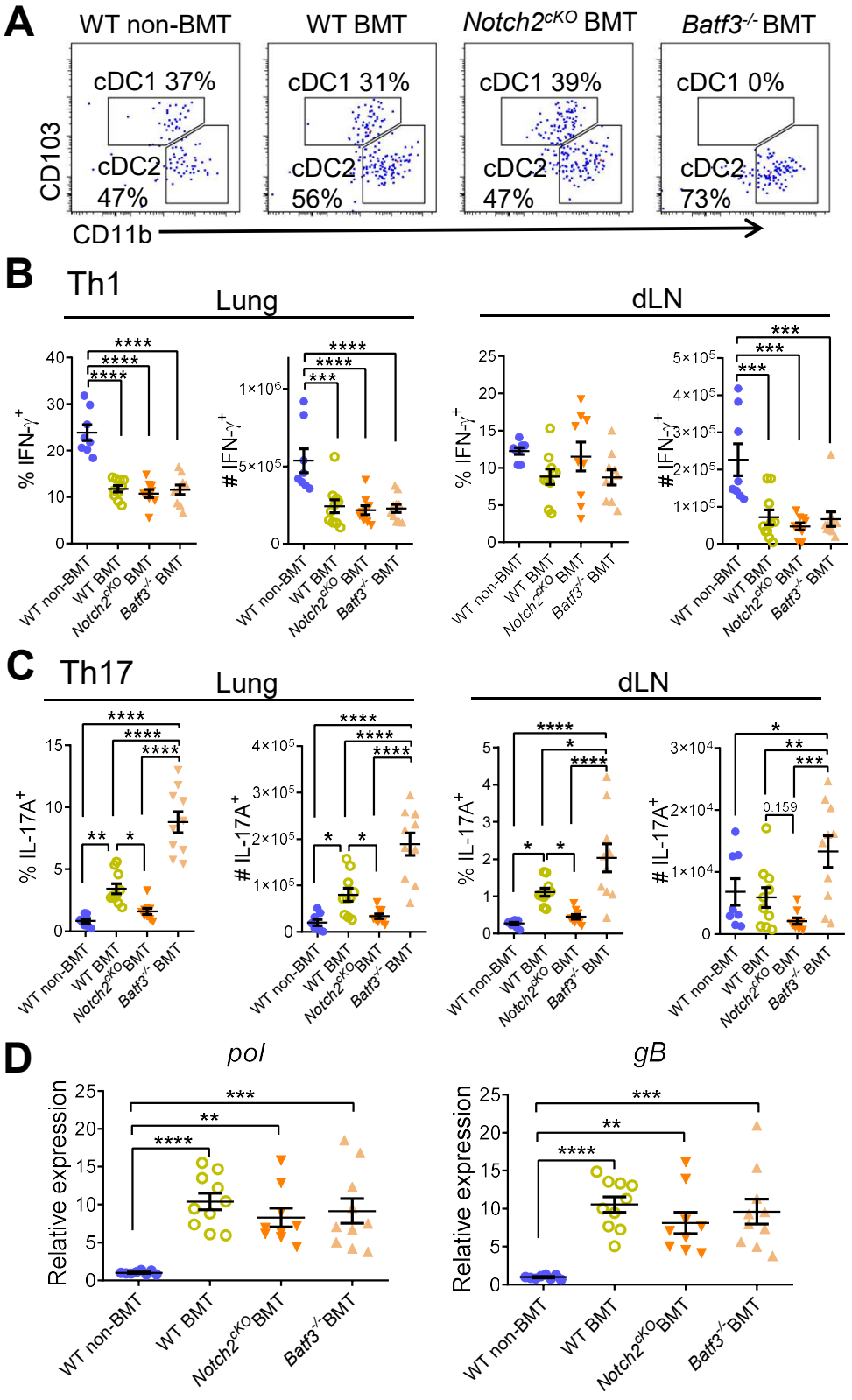
A
WT non-BMT
WT BMT
Notch2cKO BMT
Batf3-/- BMT
cDC1 37%
cDC2 47%
cDC1 31%
cDC2 56%
cDC1 39%
cDC2 47%
cDC1 0%
cDC2 73%
CD103
CD11b
B
Th1
Lung
dLN
% IFN-γ+
# IFN-γ+
C
Th17
% IL-17A+
# IL-17A+
D
pol
gB
Relative expression
WT non-BMT
WT BMT
Notch2cKO BMT
Batf3-/- BMT

Figure 5. *Notch2* function in cDC2 is required for Th17 response while *Batf3*-dependent cDC1s suppress Th17 response in BMT mice after infection with MHV-68. (A) Representative two-color histograms for CD103 and CD11b expression were gated for cDC1 or cDC2 cells in the lungs from age-matched WT non-BMT mice, or BMT mice that received bone marrow cells from WT, *Notch2*^{cKO} or *Batf3*$^{-/-}$ mice. cDCs are pre-gated as shown in Fig. 2A. Numbers indicate the percentage of cells in the gate. **(B)** Percent and absolute numbers of IFN-γ^+ Th1 cells among CD4$^+$ T cells (pregated for CD45$^+$CD90.2$^+$CD3$^+$CD4$^+$) per lung or dLN determined by flow cytometry and total cell numbers (Mean ± SEM). **(C)** Percent and absolute numbers of IL-17A$^+$ Th17 cells among CD4$^+$ T cells (pregated for CD45$^+$CD90.2$^+$CD3$^+$CD4$^+$) per lung or dLN determined by flow cytometry and total cell numbers (Mean ± SEM). **(D)** Relative mRNA abundance of viral *pol* gene (right) or *gB* (left) gene in lung tissues (Mean ± SEM). In (B), (C) and (D), lungs and dLNs were of non-BMT (n=8) or BMT mice that received bone marrow cells from WT (n=10), *Notch2*^{cKO} (n=9) or *Batf3*$^{-/-}$ (n=10) mice. Symbols represent individual mouse data points. Data were pooled from two independent experiments. * $P < 0.05$, ** $P < 0.01$, *** $P < 0.001$, **** $P < 0.0001$, one-way ANOVA followed by a Tukey's multiple comparisons test. BMT, bone marrow transplantation; cDC1, type 1 conventional dendritic cell; cDC2, type 2 conventional dendritic cell; dLN, draining lymph node.

Figure 6

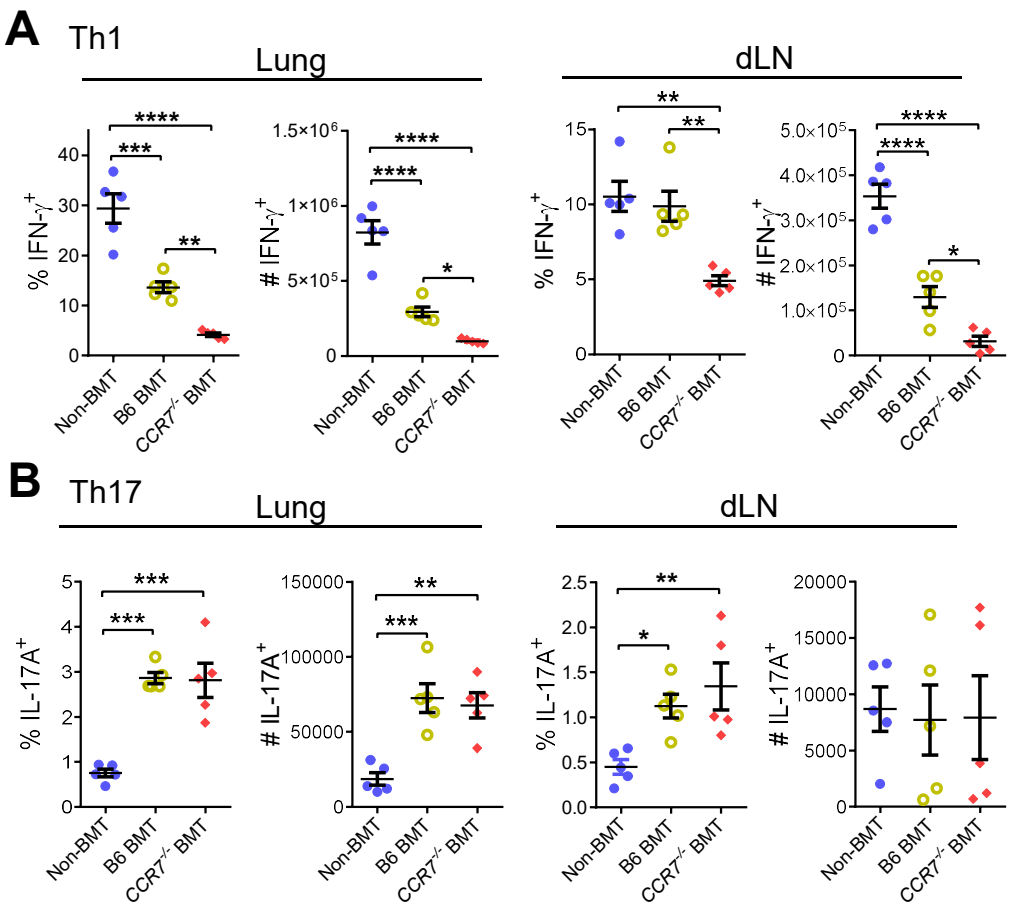

Figure 6. Migration of cDCs is essential for Th1 responses but not for Th17 responses. Live single lung cells prepared from non-BMT mice or BMT mice receiving B6 or *CCR7*$^{-/-}$ bone marrow (n=5 for each group) were pre-gated for Th cells (CD45^{+}CD3^{+}CD90.2^{+}CD4^{+}). **(A)** Percent and absolute numbers of IFN-γ^{+} Th1 cells among CD4^{+} Th cells per lung of B6 non-BMT, B6 BMT or *CCR7*$^{-/-}$ BMT mice. **(B)** Percent and absolute numbers of IL-17A^{+} Th17 cells among CD4^{+} Th cells per lung of B6 non-BMT, B6 BMT or *CCR7*$^{-/-}$ BMT mice. Symbols represent individual mouse data points. Mean ± SEM is shown for all panels. Data are representative of two independent experiments. * $P < 0.05$, ** $P < 0.01$, *** $P < 0.001$, **** $P < 0.0001$, one-way ANOVA followed by a Tukey's multiple comparisons test. BMT, bone marrow transplantation; dLN, draining lymph node.

Table 1. Primers and Probes for quantitative Real-Time RT-PCR

Gene (ref.)	Oligo	Primer sequence
MHV-68 *pol* (86)	Forward	5'-ACAGCAGCTGGCCATAAAGG-3'
	Reverse	5'-TCCTGCCCTGGAAAGTGATG-3'
	Probe	5'-CCTCTGGAATGTTGCCTTGCCTCCA-3'
MHV-68 *gB* (86)	Forward	5'-CGCTCATTACGGCCCAAA-3'
	Reverse	5'-ACCACGCCCTGGACAACTC-3'
	Probe	5'-TTGCCTATGACAAGCTGACCACCA-3'
GAPDH (88)	Forward	5'-GGGCCACGCTAATCTCATTT-3'
	Reverse	5'-ATACGGCCAAACCGTTCAC-3'
	Probe	5'-CTCCTCGAGCCTCGTCCCGT-3'
IL-23 p19 (24)	Forward	5'-CTCCCTACTAGGACTCAGCCAACT-3'
	Reverse	5'-ACTCAGGCTGGGCATCTGTT-3'
	Probe	5'-AGCCAGAGGATCACCCCCGGG-3'
IL-6 (89)	Forward	5'-GACTTCCATCCAGTTGCCTTCT-3'
	Reverse	5'-CTGTTGGGAGTGGTATCCTCTGT-3'
	Probe	5'-TGACAACCACGGCCTTCCCTACTTCA-3'
IL-12 p35 (24)	Forward	5'-GTTGCCTGGCTACTAGAGAGACTTC-3'
	Reverse	5'-GCACAGGGTCATCATCAAAGAC-3'
	Probe	5'-ACAACAAGAGGGAGCTGCCTGCC-3'
Ccl21a (90)	Forward	5'- ATGGCTCAGATGATGACTCTGAGC -3'
	Reverse	5'- GTACTTAAGGCAGCAGTCCTGA-3'
	Probe	5'- AGCCTGGTCCTGGCTCTCTGCATCC -3'

Ccl21b/c (90)	Forward	5'-AGGCAGTGATGGAGGGGGA-3'
	Reverse	5'-GCTTAGAGTGCTTCCGGGGTA-3'
	Probe	5'-TTCTTGCTTCCTATAGCCTCGGACAATACTGTAGG-3'
Ccl19 (91)	Forward	5'-CTTCCGCATCATTAGCACCC -3'
	Reverse	5'-TCATTAGCACCCCCCAGAGT-3'
	Probe	5'-TGGACCTTCCCAGCCCCAACTCTG-3'